applied sciences

MDPI

Article

Alginate-Based Patch for Middle Ear Delivery of Probiotics: A Preliminary Study Using Electrospray and Electrospinning

Beatrice Cecchini [1,†], Roberta Rovelli [1,†], Lorenzo Zavagna [2], Bahareh Azimi [1,3], Teresa Macchi [3], Esingül Kaya [3], Semih Esin [3], Luca Bruschini [4], Mario Milazzo [1,*], Giovanna Batoni [3] and Serena Danti [1,*]

[1] Department of Civil and Industrial Engineering, University of Pisa, 56122 Pisa, Italy
[2] PEGASO Doctoral School of Life Sciences, University of Siena, 53100 Siena, Italy
[3] Department of Translational Research and New Technologies in Medicine and Surgery, University of Pisa, 56126 Pisa, Italy
[4] Department of Surgical, Medical, Molecular Pathology and Emergency Medicine, University of Pisa, 56126 Pisa, Italy
* Correspondence: mario.milazzo@unipi.it (M.M.); serena.danti@unipi.it (S.D.)
† These authors contributed equally to this work.

Featured Application: Our work shows the application of electrospinning and electrospray to develop a tympanic membrane patch based on alginic acid, aimed at delivering probiotics and/or postbiotics to the middle ear. The possibility of contrasting chronic infections using probiotics is an emerging strategy, proposed as an alternative to antibiotics. Middle ear bacteriotherapy mediated by a probiotic/alginate patch can open new therapeutic routes in otology for those patients with chronic otitis media.

Abstract: Antimicrobial resistance poses a growing challenge in respiratory tract diseases like otitis media, often necessitating surgical interventions due to pharmacological treatment limitations. Bacteriotherapy, involving probiotics and/or their bioproducts, emerges as a promising alternative in such a scenario. This study aims to pave the way to middle ear bacteriotherapy by developing an innovative sodium alginate (SA)-based probiotic delivery system using electrospinning and electrospray techniques. Electrospray enabled the precise production of probiotic-laden SA microparticles, demonstrating potential for targeted bacterial delivery. By overcoming challenges due to the SA molecular structure, we successfully electrospun SA-based fiber meshes with poly(ethylene oxide) (PEO) as a support polymer. The rheologic behavior of the probiotic/SA solutions and the morphology of the obtained microparticles and fibers was evaluated, along with the diameter variation over time. The cytocompatibility of the produced microparticles and fibers was assessed using human dermal keratinocytes and their antimicrobial activity was tested against *E. coli*. The incorporation of probiotic-laden SA microparticles within electrospun SA/PEO fiber meshes finally offered a patch-like structure to be applied on the tympanic membrane or on the outer auditory canal, which could be a versatile and ideally safe treatment strategy in chronic otitis media. This innovative approach holds promise for clinical applications dealing with inflammatory processes, infections and dysbiosis, thus possibly addressing the complex healing process of chronic upper respiratory diseases while mitigating antimicrobial resistance.

Keywords: additive manufacturing; bacteriotherapy; fiber meshes; encapsulation; eardrum

Citation: Cecchini, B.; Rovelli, R.; Zavagna, L.; Azimi, B.; Macchi, T.; Kaya, E.; Esin, S.; Bruschini, L.; Milazzo, M.; Batoni, G.; et al. Alginate-Based Patch for Middle Ear Delivery of Probiotics: A Preliminary Study Using Electrospray and Electrospinning. *Appl. Sci.* **2023**, *13*, 12750. https://doi.org/10.3390/app132312750

Academic Editors: Chaoqun Dong and Xiaoming Tao

Received: 5 November 2023
Revised: 17 November 2023
Accepted: 26 November 2023
Published: 28 November 2023

Correction Statement: This article has been republished with a minor change. The change does not affect the scientific content of the article and further details are available within the backmatter of the website version of this article.

1. Introduction

Otitis media (OM) refers to inflammation and/or infection in the middle ear and encompasses a continuum of acute and chronic diseases, clinically characterized by fluid effusion in the middle ear [1]. OM is one of the most common infectious diseases in childhood and the leading cause for medical consultations, as well as antibiotic prescription in this population [2]. Complications, in time, include conductive hearing loss and severe

sequels, such as mastoiditis, cholesteatoma, meningitis, brain abscess and lateral sinus thrombosis [3,4]. OM treatment and prevention continues to provide a great challenge for researchers and clinicians, due to the current alarming spread of multidrug-resistant bacterial strains [5,6]. Thus, the identification of innovative antimicrobial strategies that can replace or complement the use of antibiotics represents a widely recognized priority [7].

In this regard, an emerging field of research aims to treat and prevent OM using bacteriotherapy, i.e., the use of beneficial bacteria or their related biological products (e.g., probiotics, postbiotics) for competing with otopathogens to contrast their growth, virulence factors and ability to induce chronic inflammation and tissue injury, e.g., eardrum perforation [8]. However, supporting data for this type of intervention are still scarce and demand for a rational and evidence-based selection of potential devices is low. In fact, adequate systems for the delivery of probiotics to the target site are not yet established [9].

In recent years, electrospinning and electrospray have emerged as suitable biofabrication techniques to produce micro/nanometric fibers and particles, which can be loaded with a wide range of molecules and live cells [10]. Microfiber and nanofiber-based technologies are of growing interest in many biomedical fields, including tympanic membrane patches as drug delivery systems [11,12]. The high surface area-to-volume ratio and high porosity of these fibrous meshes make them candidates for delivery and sustained release at the target site of the active cargos, which can be encapsulated in the fibers and/or in particles electrosprayed on the fibrous mesh [11–13].

Recently, supporting data describing bacteria encapsulation via electrospinning have also become available [14]. Bacteria were electrospun into water soluble polymers for a range of biomedical and agricultural applications. For example, *Staphylococcus epidermidis* was loaded into carboxymethyl cellulose/polyethylene oxide (PEO) fibers to treat diabetic foot ulcers [15]. In a similar fashion, *Lactobacillus acidophilus* was incorporated into poly(vinyl alcohol) (PVA)/poly(vinyl pyrrolidone) fibers to treat bacterial vaginosis [16]. The electrospinning apparatus can be used both to obtain continuous fibers and to have the feeding solution broken into droplets, thus forming micro/nano particles [12]. Owing to its mild operating conditions, electrospray has the potential to be used for the encapsulation of live cells inside biopolymeric networks forming particulate systems. Therefore, it can be considered as a method for bacteria delivery and release at a designated site in the body. Zaeim et al. used electrospray to fabricate hydrogel microspheres for encapsulation of probiotics (i.e., *Lactobacillus plantarum*) [17]. Thus, the electrospinning technology is a versatile and straightforward platform to have fiber meshes combined with particle systems [12].

A different approach is represented by three-dimensional (3D) printing, in which bacteria could be encapsulated in polymeric inks ejected via a miniaturized nozzle through the application of a pressure. 3D printing is indeed a valuable approach to fabricate 3D structures for different biomedical applications (e.g., patches for wound healing). On the one hand, 3D printing might solve the problem related to the swelling of fibers observable in electrospinning applications by a careful control of the process parameters (i.e., temperature, deposition velocity, viscosity of the ink) [18]. However, the size of the printed filaments and the weight of the produced structures would be higher than those obtainable via electrospinning, which could limit eardrum hearing function.

Among water soluble polymers, necessary to support cell viability, natural polysaccharides are outstanding figures, as they can retain very large amounts of water useful for the embodied cells, and are entitled with low immunogenicity and high biocompatibility towards different tissues of the body [19,20]. A key example is alginic acid, a natural anionic polysaccharide derived from brown seaweeds (i.e., *Phacophycae*), which has gained a long-term growing appreciation in drug delivery systems and other biomedical applications due to its key properties, including its structural similarity to the amorphous extracellular matrix in tissues [21]. Alginic acid sodium and potassium salts, known as alginates, are block-copolymer polysaccharides of L-guluronic (G) and D-mannuronic (M) acid residues connected by 1:4 glycoside linkages. Their crosslinking occurs via an exchange of monovalent cations (e.g., Na^+) to bivalent cations (e.g., Ca^{2+}), causing hydrogel formation, which is

ideal to entrap live cells and biomolecules [22]. Some examples of alginate-based platforms for bacterial encapsulation have been reported in the literature. Diep et al. developed alginate-based nanofibers that could potentially serve as a biocompatible and edible system for the safe delivery of live bacteria into the gut [23]. However, due to the strong entanglement of alginate chains, electrospun continuous fibers were obtained using a synthetic hydrophilic polymer as a carrier, such as PEO or PVA, usually in a relevant amount with respect to sodium alginate (SA) [15,16].

The present work is focused on fabricating SA probiotic electrosprayed/electrospun fiber patch as a tool to possibly treat middle ear infections via bacteriotherapy. In particular, the electrospinning technique was exploited to produce SA-based microparticles containing probiotics embedded in SA-based fibrous meshes, as a supportive substrate for the topical application in the tympanic membrane. To reach this goal, electrospray and electrospinning processes needed the alginate-based formulations to be tuned. We thus investigated the rheological properties of the SA-based solutions and the morphology of the fibers and probiotic-loaded versus unloaded microparticles. Moreover, size variation upon crosslinking, swelling and biodegradation in physiological-like medium, cytocompatibility towards epithelial cells and antimicrobial activity towards a model pathogen, *E. coli,* were studied.

2. Materials and Methods

2.1. Materials

SA suitable for cell immobilization in powder form (code 71238), low viscosity SA in powder form (code A1112) and medium viscosity SA in powder form (code A2033) were purchased from Sigma-Aldrich (Milan, Italy). The SAs used are further indicated by a "SA(M_w)MG(##)" string, in which M_w is the molecular weight (in kDa) and MG is the M/G ratio; the MG value ## is given in numbers without decimal punctuation. Information regarding the molecular weight and M/G ratio of SA427MG07 and SA495MG19 was obtained through gel permeation chromatography (GPC) and 1H-NMR, respectively, as reported by Gorroñogoitia, et al. [24]. Information regarding the molecular weight and M/G ratio of the SA51MG03 was obtained with chromatographic techniques, as reported by Jeoh et al. [25]. Poly(ethylene oxide) (PEO) in powder form with a molecular weight of 1000 kDa (code 372781), liquid Triton X-100 (Lot#110M0009V) and agar were also purchased from Sigma-Aldrich. Absolute ethanol was bought from Bio-Optica (Milan, Italy)

Probiotics (Probioti, 60 capsules) were purchased from OTI—Officine Terapie Innovative s.r.l. (Carsoli, AQ, Italy). In 4 capsules, they are reported to contain a mixture of the following live probiotic strains in colony forming units (CFUs): *Lactobacillus plantarum* BG112 > 10 bn CFUs, *Streptococcus thermophilus* SP4 > 5 bn CFUs, *Lactobacillus casei* BGP93 > 5 bn CFUs, *Lactobacillus acidophilus* LA3 > 2 bn CFUs, *Bifidobacterium breve* SP85 > 1 bn CFUs, *Bifidobacterium infantis* SP37 > 1 bn CFUs, *Bifidobacterium longum* SP46 > 1 bn CFUs and *Lactobacillus bulgaricus* SP5 > 0.25 bn CFUs.

Human Keratinocyte (HaCaT) cell line was obtained from CLS-Cells Line Service (Eppelheim, Germany). Fetal Bovine Serum (FBS) was purchased from Thermo Fisher Scientific (Waltham, MA, USA). Dulbecco's Phosphate Buffered Saline (DPBS), Dulbecco's Modified Essential Medium (D-MEM), L-Glutamine, penicillin and streptomycin were purchased from Sigma Aldrich. AlamarBlue® was purchased from Thermo Fisher Scientific. De Man-Rogose-Sharpe agar (MRSA) and Tryptic Soy Broth (TSB) were obtained from Oxoid Ltd., Cheshire, UK. *Escherichia coli* ATCC 25922 was purchased from ATCC (Manassas, VA, USA).

2.2. Preparation of SA Solutions for Electrospray

SA427MG07 was used to prepare 2 *w*/*v*% aqueous solutions in distilled water (dH_2O) for electrospray. SA427MG07 was weighed using an analytical balance and slowly poured in stirring water. Gentle stirring was kept overnight at room temperature (RT) before use. Solutions containing model commercial probiotics for preliminary investigations were prepared using the powder content of Probioti capsules, which was dissolved in dH_2O

prior to the addition of SA. The contents of 2 capsules (0.41 ± 0.01 g of powdered probiotics per capsule), corresponding to 5×10^9 live probiotics, were dissolved in 5 mL of water under stirring. Afterwards, 0.10 g of SA was slowly added to the stirring solution to achieve a final SA concentration of 2 *w*/*v*%. Gentle stirring was kept overnight at RT before use.

2.3. Preparation of SA/PEO Solutions for Electrospinning

SA(s)/PEO solutions investigated for electrospinning are detailed in Table 1.

Table 1. Water solution of sodium alginates (SAs) tested for electrospinning.

SA Type [1]	SA Concentration [*w*/*w*%]	PEO Concentration [*w*/*w*%]	SA/PEO [*w*/*w*]	Triton X Concentration [*w*/*w*%]
SA51MG03	12.0	3	80/20	1
SA51MG03 + SA495MG19	6.5 + 0.5	3	70/30	1
SA51MG03	7.0	3	70/30	1

[1] Sodium alginate (SA) type is indicated by its molecular weight (M_w, in kDa) and mannuronic/guluronic ratio (MG, in numbers without decimal punctuation), which results in a string "SA(M_w)MG(##)".

To produce fibers by electrospinning, SA solutions containing PEO as a carrier were prepared. First, SA(s) in powder form were slowly added to dH_2O and stirred at 800 revolutions per minute (rpm), 40 °C for 30 min to promote the polymer dissolution. Afterwards, PEO powder was slowly added to the SA, and kept under stirring in the same conditions for 2 h. At this point, liquid Triton X-100 was added to the solution using a pipette, and the stirring was maintained overnight at RT to ensure a complete dissolution and mixing of the components.

2.4. Rheological Analysis of Prepared Solutions

A rheological analysis was carried out to evaluate the viscosity of SA water solution (i.e., 2 *w*/*v*% SA427MG07 in dH_2O) with and without probiotics used for electrospray, as well as SA/PEO solution (i.e., 7 *w*/*w*% SA51MG03 + 3 *w*/*w*% PEO + 1 *w*/*w*% Triton X-100) used for electrospinning. Viscosity measurements were performed at 25 °C using the MC20 rheometer endowed with coaxial cylinders (Anton Paar, Rivoli, TO, Italy) and a solution volume of 17 mL. The viscosity as a function of the shear rate was then evaluated in the range 10^{-1}–10^3 Hz. The shear rate ($\dot{\gamma}$) corresponding to our electrospinning setup was evaluated by using the Hagen–Poiselle equation (Equation (1)) for capillaries and tubes:

$$\dot{\gamma} = \frac{4V}{\pi R^3 t} = \frac{4F}{\pi R^3} \quad (1)$$

in which *R* is the needle inner radius, *V* is the fluid volume, *t* is the time; therefore, *F* is the flow rate [26].

2.5. Electrospray Procedure to Obtain Probiotic-Laden Microparticles

A schematic of electrospray set-up is shown in Figure 1A. Specifically, 5 mL of 2 *w*/*v*% SA427MG07 in dH_2O solution, either with or without probiotics, was loaded into a disposable syringe equipped with a blunt end bent stainless steel 22G needle (inner diameter: 0.413 mm). The syringe was assembled onto a syringe pump (Linari Engineering s.r.l., Pisa, Italy) and the needle was connected to a high-voltage supply (Linari Engineering s.r.l.). The collector was prepared by placing an aluminum foil disc inside a Petri dish filled with 30 mL of a $CaCl_2$ solution.

A sheathed copper wire with exposed ends was placed in contact with the aluminum foil on one end and connected to the ground terminal on the other end. The electrospray was carried out for 10 min, and the microparticles were maintained in the collection bath for 10 min to achieve crosslinking. The collection bath was then transferred into a Falcon tube, and the collector was washed 3 times with 5 mL of dH_2O to recover residual microparticles.

The samples were left in the $CaCl_2$ solution overnight to complete the crosslinking process. Then, the liquid was removed using a pipette and 20 mL of dH_2O were added prior to shaking. This procedure was repeated 3 times to obtain a complete removal of the $CaCl_2$ solution.

The distance between the tip of the needle and the surface of the liquid inside the Petri dish was 9 cm. Flow rate, applied voltage and $CaCl_2$ solution concentration parameters were evaluated to identify the best electrospray conditions. First, 3 flow rates, i.e., 1 mL/h, 2 mL/h and 3 mL/h, were tested, and the microparticles were observed using an inverted optical microscope (Nikon Eclipse Ti; Nikon, Tokyo, Japan) to identify the flow rate that could yield the best microparticles in terms of shape and dimensional homogeneity. Afterwards, the same procedure was repeated by maintaining a fixed selected flow rate and testing 3 voltages: 20 kV, 22 kV and 25 kV. Finally, microparticles were produced again with the optimal flow rate and voltage parameters to compare two concentrations of the crosslinking solution: 1 w/v% and 2 w/v%.

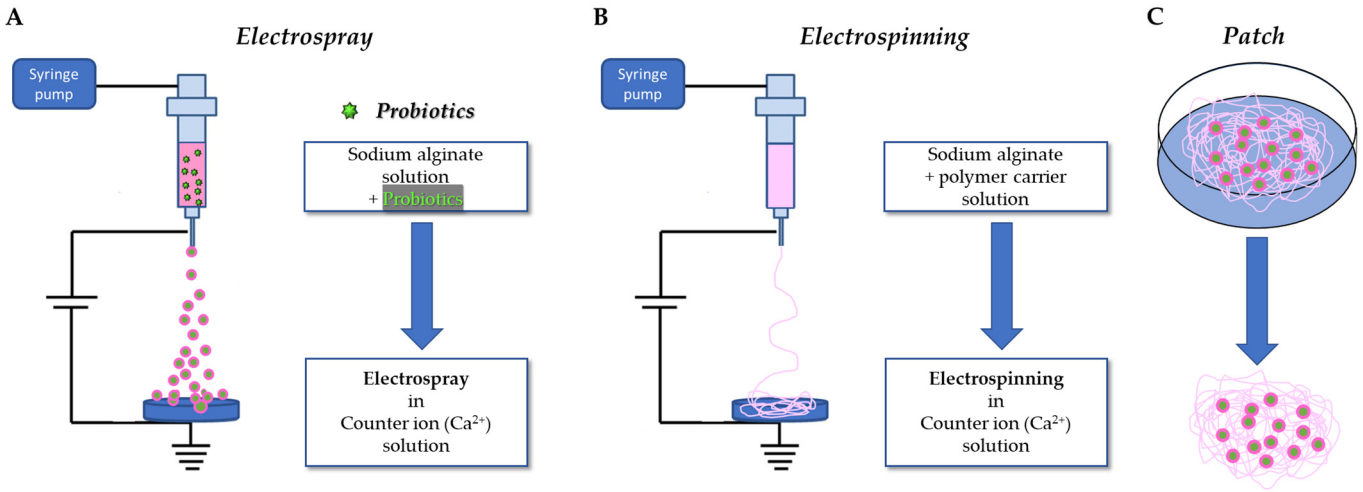

Figure 1. Schematics showing (**A**) probiotic-laden microparticle production in SA solution via electrospray; (**B**) submicrometric nanofiber production via electrospinning SA/PEO solution. Both systems are collected in a $CaCl_2$ water bath. (**C**) Assembled probiotic-laden microparticle/fiber patch.

2.6. Electrospinning Procedure to Obtain SA/PEO Fiber Meshes and the Assembled Patch

A schematic of the electrospinning set-up is displayed in Figure 1B. In detail, 5 mL of solution was loaded into a disposable syringe equipped with a blunt end stainless steel 22G needle (inner diameter: 0.413 mm). The syringe was assembled onto the same equipment described above: a syringe pump and a high-voltage supply (all from Linari Engineering s.r.l.) connected the needle using different settings. The SA/PEO solutions (reported in Table 1) were electrospun in air and crosslinked afterwards. The fibers were collected by setting the parameters as follows: a flow rate of 0.75 mL/h, a voltage of 12 kV and a needle-collector distance of 7.5 cm. Both a low rotational speed (60 rpm) and a high rotational speed (1500 rpm) were tested to achieve the formation of randomly oriented and aligned fibers, respectively. Different crosslinking conditions were tested, consisting of 30 s immersion in: (*i*) 2 w/v% $CaCl_2$ dH_2O solution; (*ii*) 2 w/v% $CaCl_2$ 30/70 v/v% ethanol/dH_2O solution; (*iii*) 30/70 v/v% ethanol/dH_2O solution, followed by 30 s immersion in 2 w/v% $CaCl_2$ dH_2O solution.

The deposition of probiotic-laden microparticles onto the SA/PEO fibrous mesh was approached as follows. After performing the electrospinning process at a collection speed of 1500 rpm and the subsequent stabilization of the fiber mesh through crosslinking, the wet fibrous sample was repositioned on the rotating drum. Therefore, the electrospray technique was employed to deposit probiotic-laden SA microparticles onto the wet fiber

mesh. The assembled patch underwent a controlled drying process before being subjected to SEM analysis (Figure 1C).

2.7. Swelling and Biodegradation

The swelling and biodegradation behavior were observed for probiotic-free microparticles and fibers. For the microparticles, the supernatant water was removed from the Falcon tube, 20 mL of DPBS was added to the microparticles and the samples were stored at 37 °C. Therefore, 20 µL of particle suspension was withdrawn for particle observation at specific time intervals, i.e., 30 min, 1 h, 2 h, 4 h, 24 h, 48 h, 72 h, 1 week, and 2 weeks. The pH of the liquid medium was measured at the same time intervals.

For the fibers, samples for each rotational speed were prepared by cutting 10 rectangles of ~2 cm^2 from the aluminum foil coated in fibers. The samples were then crosslinked for 30 s in 2 w/v% $CaCl_2$ in a water–ethanol mixture (30 v/v% ethanol in water), except for 1 sample for each rotational speed. A total of 8 crosslinked samples for each rotational speed were then submerged individually in 4 mL DPBS and stored at 37 °C for the degradation analysis. Each sample was removed from the degradation medium at specific time intervals, i.e., 30 min, 1 h, 2 h, 4 h, 24 h, 48 h, 72 h, 1 week, and the pH of the corresponding medium was measured.

2.8. Morphological Analysis of Microparticles and Fibers

Probiotic-free and probiotic-laden electrosprayed microparticles were observed using an inverted optical microscope (Nikon Eclipse Ti, Nikon, Japan). The watery suspension of microparticles was shaken, 20 µL was withdrawn with a Gilson pipette and deposited on a Petri dish for observation. The fibers were dried in air at RT for 24 h; thereafter, appropriately sized samples were mounted on stubs and gold sputtered using a sputter coater Edwards S150B (Edwards Italy, Cinisello Balsamo, MI, Italy) for 3 min. The fiber samples were observed using Coxem EM-30^N Scanning Electron Microscope (SEM) (Daejeon, Republic of Korea). All samples were observed at different magnifications using a high voltage of 15 kV and the secondary electrons mode.

The diameters of probiotic-free and probiotic-laden microparticles (n = 50) obtained via inverted microscopy and those of the fibers (n = 50) obtained by SEM were measured using ImageJ-3 (ImageJ 1.53a Wayne Rasband National Institutes of Health, Bethesda, MD, USA). The eccentricity of probiotic-free and probiotic-laden microparticles (n = 50) was measured using Equation (2), in which a and b are the semi axes of an ellipsoidal particle:

$$e = \sqrt{\frac{a^2 - b^2}{a^2}} \quad (2)$$

2.9. Cytocompatibility

Human dermal keratinocytes (i.e., HaCaT cells) were used as a model of eardrum outer epithelium to conduct in vitro indirect cytotoxicity tests. The biomaterial samples were prepared to have a uniform weight of 0.1 g each, and were placed in a 24-well plate and sterilized with UV for 1 h. Thereafter, 2 mL of D-MEM was added to the wells. The samples were incubated with D-MEM at 37 °C and 5% CO_2/95% humidified air conditions for 24 h. HaCaT cells, seeded in 24-well plates at a density of $15 \cdot 10^4$ cells/well until 80% of confluence, were incubated for 48 h with the culture media put in touch with the biomaterial samples (n = 3), in the incubator at 37 °C. At the end of this time, cell metabolic activity was evaluated using the AlamarBlue® assay, according to the manufacturer's instructions. We used the protocol for cytotoxicity, i.e., calculated against positive controls, with the same numericity as samples', which are obtained by adding the dye solution to the mere cells. Briefly, AlamarBlue® incorporates a redox indicator that changes its color according to cell metabolic activity.

Samples and controls were incubated for 3 h at 37 °C with the AlamarBlue® dye diluted in culture media according to the manufacturer's instructions. At each time-point,

100 µL of supernatant, obtained from the sample or control, was loaded in a well of a 96-well plate; excess supernatant was removed from the cultures and replaced with fresh culture media. The supernatants were analyzed with a spectrophotometer Victor 3 (PerkinElmer, Waltham, MA, USA), using a double wavelength reading at 570 nm and 600 nm. Finally, the reduced percentage of the dye (AB_{red}%) was calculated by correlating the absorbance values and the molar extinction coefficients of the dye at the selected wavelengths. The calculation is performed using Equation (3), in which λ = absorbance, s = sample, and c = control:

$$AB_{red}\% = 100 \times \frac{117.216 \cdot \lambda_{s(570\ nm)} - 80.586 \cdot \lambda_{s(600\ nm)}}{117.216 \cdot \lambda_{c(570\ nm)} - 80.586 \cdot \lambda_{c(600\ nm)}} \quad (3)$$

2.10. Evaluation of Antimicrobial Activity

Empty or probiotic-loaded microparticles were resuspended in sterile water at 75 mg/mL and 50 µL of the microparticle suspension was placed in triplicate on the center of 90 mm Petri dishes containing 15 mL MRSA. Plates were incubated for 24 and 72 h at 37 °C. Soft agar was prepared by adding 0.5% agar in TSB. An overnight culture of *E. coli* was diluted in TSB until an optical density at 600 nm of 0.1 was obtained. *E. coli* suspension was inoculated in TSB soft agar at 50 °C by diluting 50 times to reach a final bacterial concentration of approximately 10^6 CFU/mL. Therefore, 10 mL of TSB-soft agar was carefully overlaid on pre-incubated MRSA seeded with microparticles. After solidification of the overlaid agar medium at RT, plates were further incubated for 18 h at 37 °C. The diameters of the inhibition zones were measured and interpreted as proposed by Shokryazdan et al. [27]: diameters > 20 mm, 10–20 mm and < 10 mm were considered as strong, intermediate and weak inhibitions, respectively.

2.11. Statistical Analysis

Statistical analysis was carried out using the independent Student's *t*-test and one-way ANOVA test for morphological characterizations and biological assays. Data were analyzed by Jamovi Software (v. 2.2.5.), taking account of the numerosity (n) of the samples and setting a significance probability threshold (p) equal to 0.05. All data are represented as mean standard ± deviation.

3. Results

3.1. Rheological Analysis of SA-Based Solutions

The rheological analysis of SA-based solutions is reported in Figure 2. At RT, the SA solutions displayed a pseudoplastic behavior at low shear rates ($\leq$28 s^{-1}), which was particularly evident in the SA solution containing probiotics used for electrospray and in the SA/PEO solution used for electrospinning (Figure 2B,C). By using the Hagens–Poiseuille equation (Equation (1)), a shear rate of 30 s^{-1} was obtained for the electrospinning solution. This value exceeded the upper limit of the pseudoplastic range (Figure 2C), indicating the solution adherence to Newtonian behavior, which is a fundamental requirement for successful electrospinning. At higher shear rates (100–1000 s^{-1}), the viscosity became constant (6.52 × 10^{-3} Pa·s), thus the solution was behaving as a Newtonian fluid.

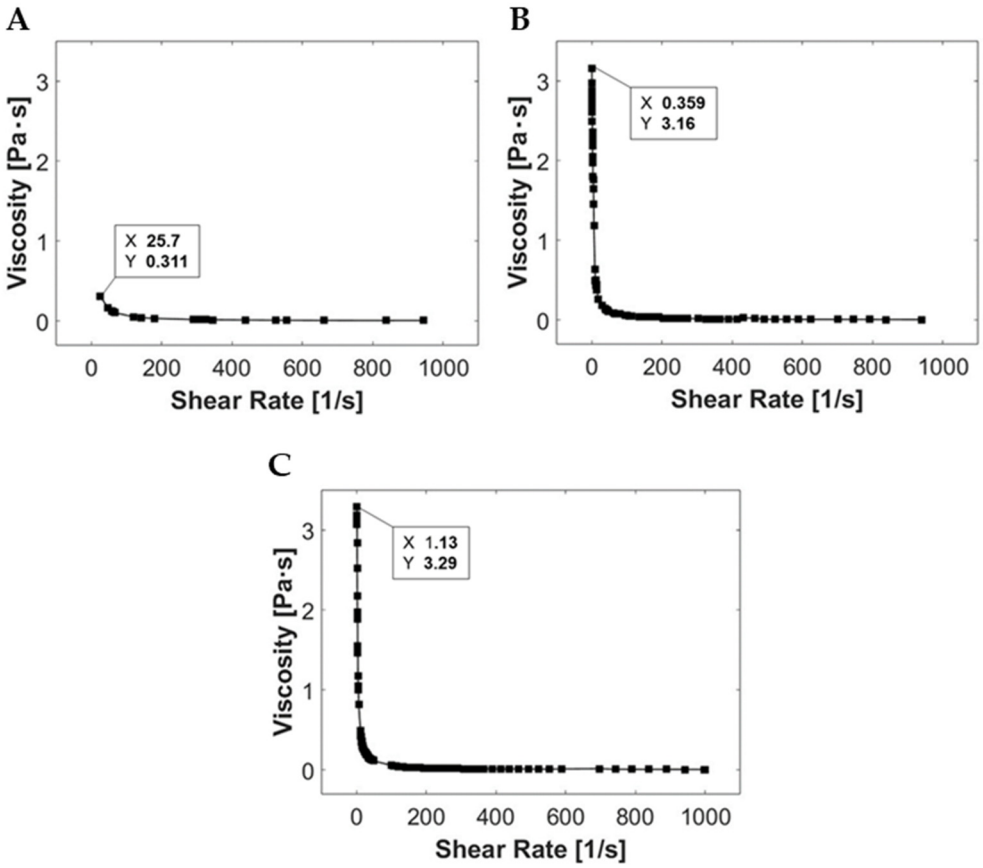

Figure 2. Plots showing the results of viscosity as a function of the shear rate. (**A**,**B**) Electrosprayed SA water solutions: (**A**) probiotic free, (**B**) probiotic laden. (**C**) Electrospun SA/PEO water solution.

3.2. Elelctrospray Procedure and Morphological Analysis of SA Microparticles

The optimized electrospray procedure, namely, with a flow rate of 3 mL/h, a voltage of 22 kV and a needle-collector distance of 9 cm, led to the obtainment of homogeneous size microparticles (Figure 3A,B). To confirm the presence of probiotics in the microparticles by inverted light microscopy, plain probiotics were also imaged (Figure 3D). As produced, probiotic-free microparticles exhibited a spherical shape with 346 ± 10 μm diameter, whereas probiotic-laden microparticles had a 395 ± 23 μm diameter with a slight elliptical shape (eccentricity of 0.43 ± 0.17 μm), which resulted in a statistical difference in size ($p < 0.001$) (Figure 3C).

After 2 h in simulated body fluid conditions, namely DPBS at 37 °C, a maximum swelling occurred, leading to a particle size of 421.6 ± 15.5 μm; thereafter, an equilibrium was reached at 392.8 ± 13.7 μm diameter, which was observed for up to 14 days (Figure 4). This test demonstrated the good stability of the microparticles over time.

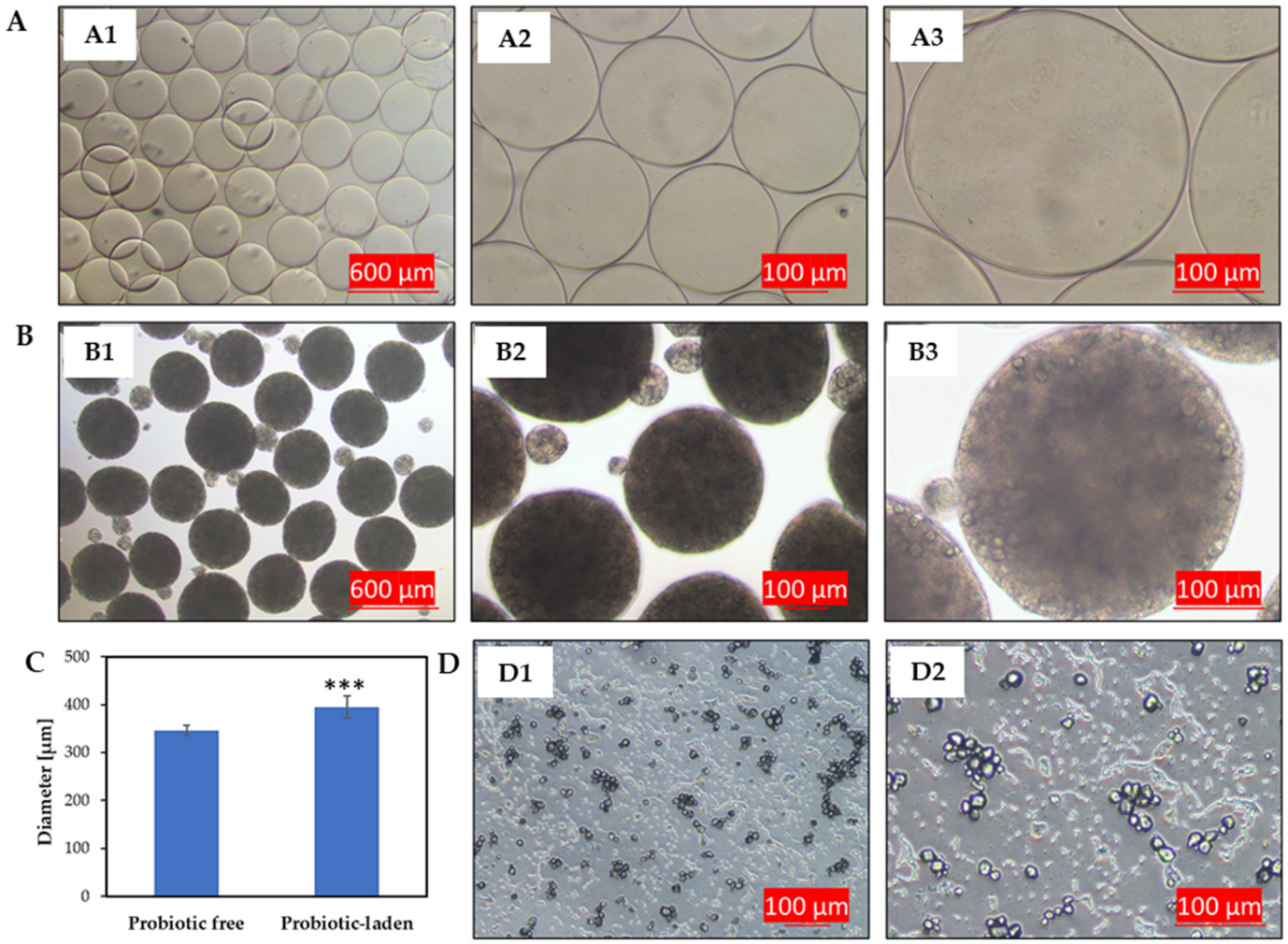

Figure 3. (**A**) Probiotic-free and (**B**) probiotic-laden SA microparticles acquired at (**A1**,**B1**) 4×, (**A2**,**B2**) 10× and (**A3**,**B3**) 20× magnifications; and (**D**) plain probiotics in water acquired at (**D1**) 10× and (**D2**) 20× magnifications. (**C**) Bar graph showing the diameters of probiotic-free versus probiotic-laden SA microparticle. Data are expressed as mean ± standard deviation. Statistical analysis was performed with a *t*-test; *** p-value ≤ 0.001.

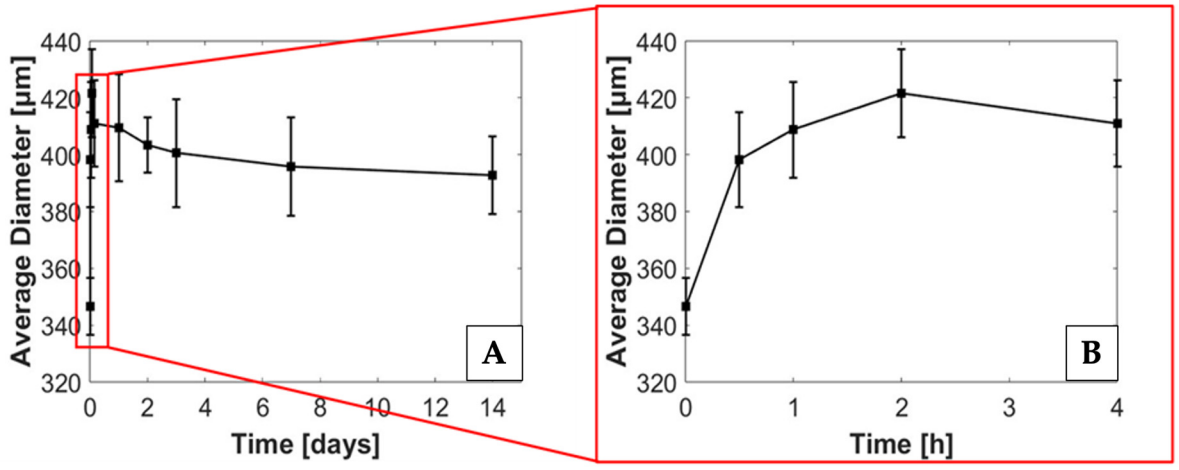

Figure 4. (**A**,**B**) Plots showing the diameter variations of SA microparticles during the biodegradation test: (**A**) complete time span of 14 days, (**B**) focus on the first 4 h.

3.3. Electrospinning Procedure and Morphological Analysis of SA/PEO Fiber Meshes

Out of the three SA/PEO solutions evaluated for electrospinning (Table 1), the formulation based on 7 *w*/*w*% SA51MG03 (i.e., 7 *w*/*w*% SA51MG03 + 3 *w*/*w*% PEO + 1 *w*/*w*% Triton X-100) proved optimal for fiber fabrication. This solution successfully produced solid, cylindrical ultrafine fibers at both 60 rpm and 1500 rpm collector speeds, as confirmed by SEM micrographs (Figure 5(A1,B1)).

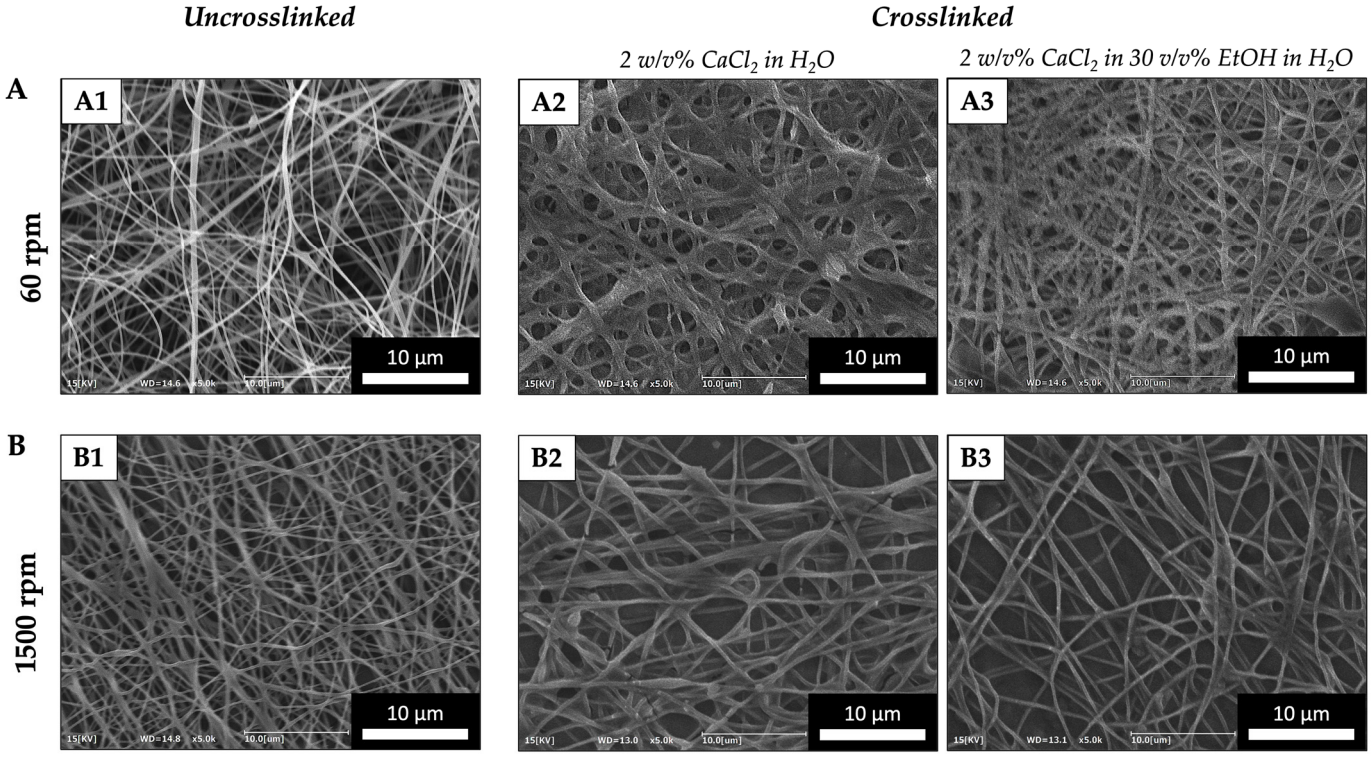

Figure 5. SEM micrographs of (**A1**) uncrosslinked and (**A2**,**A3**) crosslinked SA/PEO fibers electrospun at 60 rpm, acquired at 5000× magnification (**A2**: crosslinking in 2 *w*/*v*% $CaCl_2$ in H_2O; A3: crosslinking in 2 *w*/*v*% $CaCl_2$ in 30 *v*/*v*% EtOH in H_2O) and 15 kV. SEM micrographs of (**B1**) uncrosslinked and (**B2**,**B3**) crosslinked SA/PEO fibers electrospun at 1500 rpm, acquired at 5000× magnification (**B2**: crosslinking in 2 *w*/*v*% $CaCl_2$ in H_2O; B3: crosslinking in 2 *w*/*v*% $CaCl_2$ in 30 *v*/*v*% EtOH in H_2O) and 15 kV.

Notably, the 1500 rpm collector speed resulted in superior fiber alignment and slightly larger diameters (d = 281 ± 79 nm) compared to 60 rpm speed (d = 264 ± 95 nm). Upon subjecting the SA/PEO solution to crosslinking, significant changes in fiber morphology were observed, as illustrated in Figure 5. Methods (*i*) (2 *w*/*v*% $CaCl_2$ dH_2O solution) and (*ii*) (2 *w*/*v*% $CaCl_2$ 30/70 *v*/*v*% ethanol/dH_2O solution) allowed fibers to form welds at intersection points, leading to an interlocked network, and increasing fiber diameter. Method (*i*) induced a more pronounced diameter increase (60 rpm: d = 443 ± 15 nm; 1500 rpm: d = 450 ± 66 nm) compared to method (*ii*) (60 rpm: d = 404 ± 10 nm; 1500 rpm: d = 434 ± 92 nm), regardless the collector speed, while crosslinking strategy (*ii*) led to an increased density of welds at fiber intersection points. In contrast, method (*iii*) 30/70 *v*/*v*% ethanol/dH_2O solution) had a dramatic impact, resulting in the complete fusion of fiber structures and the formation of films (not shown). The structural stability of the ionically crosslinked SA/PEO fibers via method (*ii*) was examined by incubation in simulated biological conditions (Figure 6). After 24 h, the fibers collected at 60 rpm exhibited a diameter of 853 ± 22 nm, while those at 1500 rpm had a diameter of 666 ± 14 nm. These results demonstrated a statistically significant increase in fiber diameter over the 24 h period, indicating ongoing swelling (Figure 7).

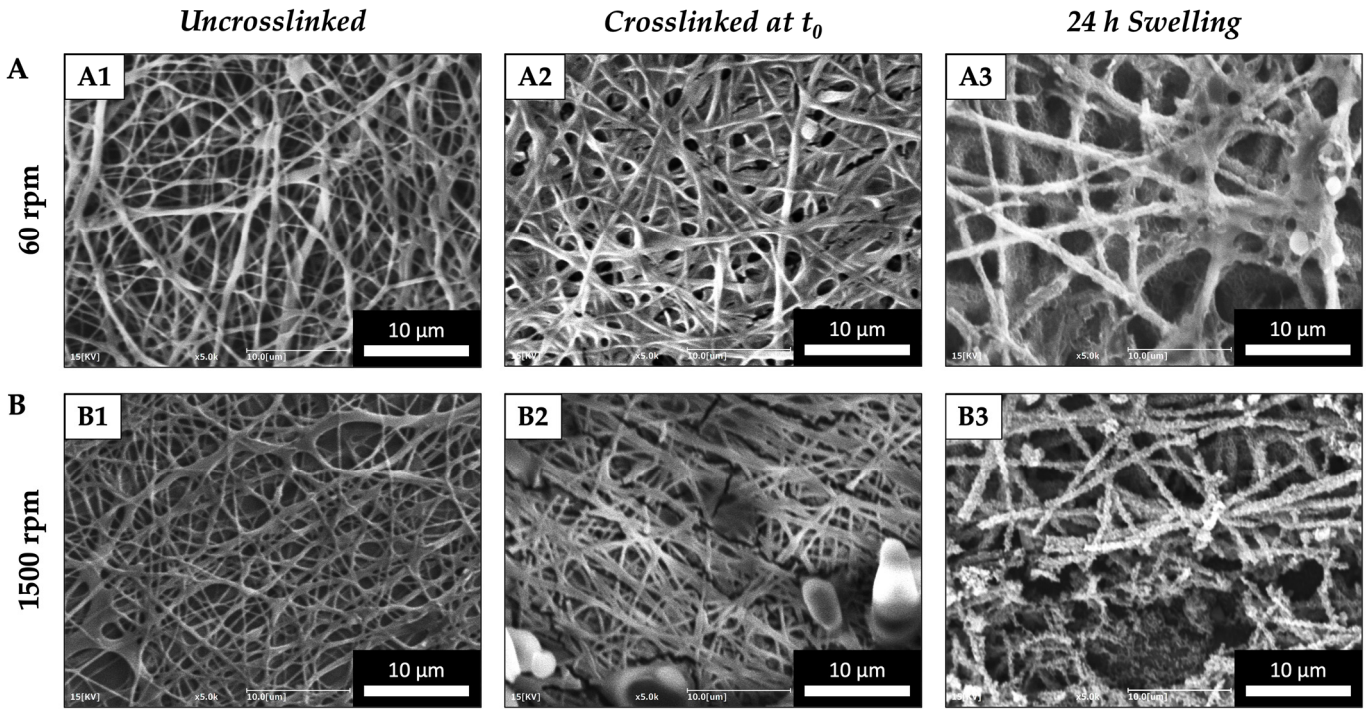

Figure 6. SEM micrographs of (**A1**) uncrosslinked and (**A2**) crosslinked SA/PEO fibers, and (**A3**) SA/PEO fibers after 24 h in the biodegradation medium collected at 60 rpm and acquired at 5000× and 15 kV. SEM micrographs of (**B1**) uncrosslinked, (**B2**) crosslinked SA/PEO fibers, and (**B3**) SA/PEO fibers after 24 h in the biodegradation medium collected at 1500 rpm and acquired at 5000× and 15 kV.

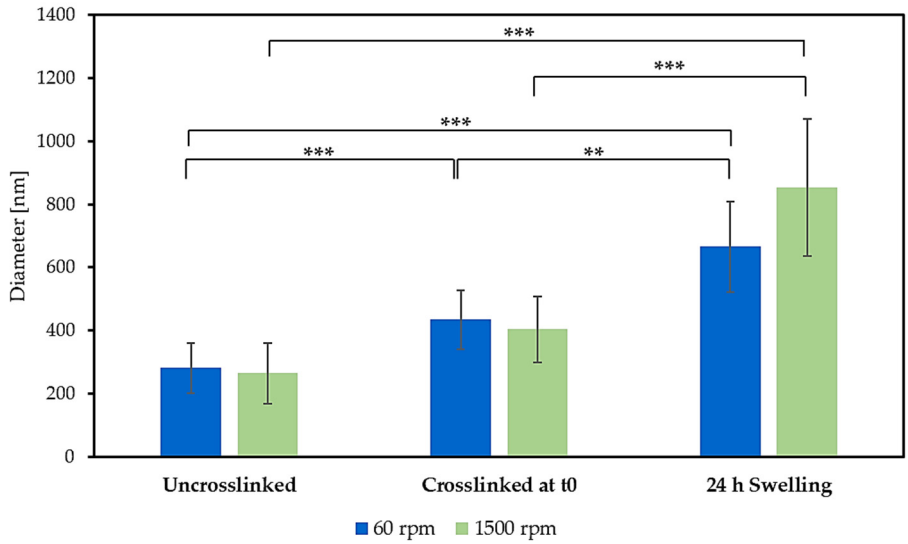

Figure 7. Bar graph showing the diameter of SA/PEO fibers collected at 60 rpm and 1500 rpm, at different process steps (i.e., uncrosslinked at t_0, crosslinked at t_0 and after 24 h) of the biodegradation test. Data are expressed as mean ± standard deviation. Statistical analysis was performed via ANOVA; ** p-value ≤ 0.01. *** p-value ≤ 0.001.

3.4. Cytocompatibility

The results of the AlamarBlue® test for electrosprayed SA microparticles and electrospun SA/PEO fibers are shown in Figure 8. Both microparticles and fibers were demonstrated to keep the normal metabolic activity in HaCaT cells after 48 h, with no statistically significant difference between the two groups (p = n.s.). On average, the results indicated a

neutral (102.46% for SA microparticles) to a slightly positive (112.24% for SA/PEO fibers) effect of the biomaterial extracts on cell metabolic activity.

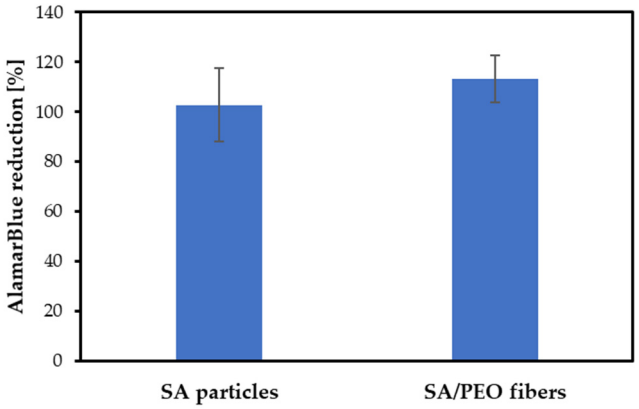

Figure 8. Bar graph showing the results of metabolic activity of HaCaT cells, evaluated as resazurin reduction percentage (AB_{red}%) using AlamarBlue assay, after 48 h of indirect contact with SA microparticles and SA/PEO fibers collected at 1500 rpm. The assay was performed against positive controls (i.e., cells without biomaterial extract). Data are expressed as mean ± standard deviation. Statistical analysis was performed via Student *t*-test; not significant (n.s.) = *p*-value > 0.05.

3.5. Integration of Probiotic-Laden Microparticles into SA/PEO Fiber Meshes

After successfully fabricating SA microparticles and SA/PEO fiber meshes, these items were combined in the attempt to develop SA-based probiotic-laden microparticles embedded in SA-based fibrous meshes, to act as a locally applicable tool for treating middle ear infections via bacteriotherapy. The assembling approach used to produce the patch ensured an optimal adherence during the crosslinking of the microparticles, which was facilitated by the diffusion of the crosslinking solution within the wet fiber mesh. SEM micrographs (Figure 9(A1,A2)) confirmed the integration of SA probiotic-laden microparticles at the surface of the fibers collected at 1500 rpm. Notably, at higher magnification, i.e., 5000×, probiotics can be visualized on the surface of the microparticles, providing further evidence of their presence (Figure 9(A2)).

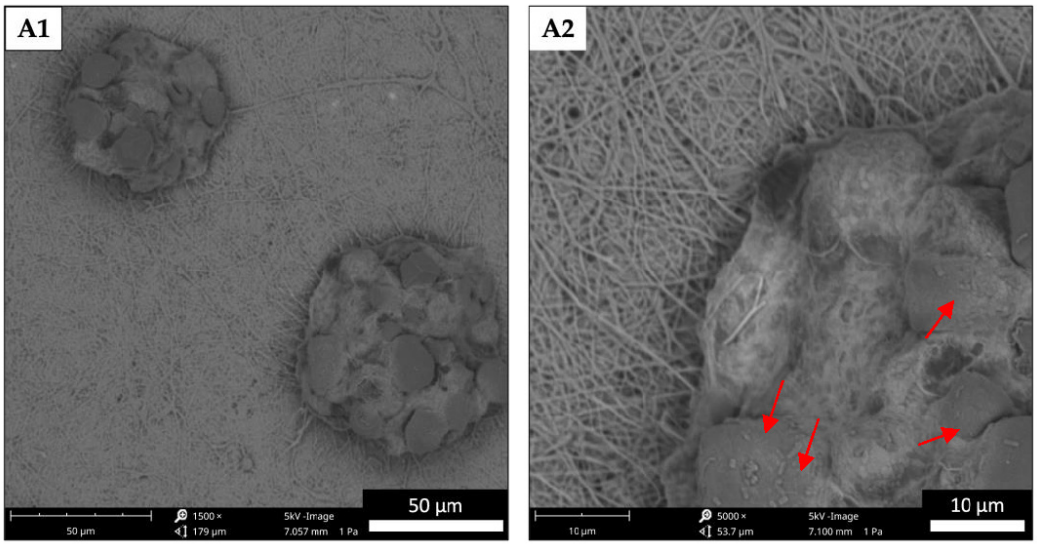

Figure 9. SEM micrographs of SA microparticles electrosprayed on SA/PEO fibers collected at 1500 rpm, acquired at different magnifications (**A1**: 1500×; **A2**: 5000×) and 15 kV. (**A2**): arrows point to bacteria on the surface of the microparticles.

3.6. Inhibition of E. coli Growth by Probiotic-Laden Microparticles

The ability of probiotic-loaded microparticles to inhibit the growth of a laboratory strain of *E. coli* was assessed by a standard soft agar overlay method. To this aim, the microparticles were spot inoculated on the surface of a nutrient medium and incubated for 24 h and 72 h at 37 °C, to let probiotics grow and release their array of antimicrobial substances all around the inoculation zone. After overlaying the *E. coli* containing soft agar medium, and further incubating the plates at 37 °C, an evident growth inhibition zone was visible as a clear halo around the probiotic-loaded microparticles (Figure 10A,B). In contrast, no inhibition zone was observed in the control plates inoculated with empty microparticles (Figure 10C). As shown in Figure 10D, the inhibitory effect was time dependent, as demonstrated by the statistically significant increase in the diameter of the inhibition zone between 24 h and 72 h ($p < 0.001$). At both 24 h and 72 h, the inhibitory effect was classified as "strong", i.e., >20 mm.

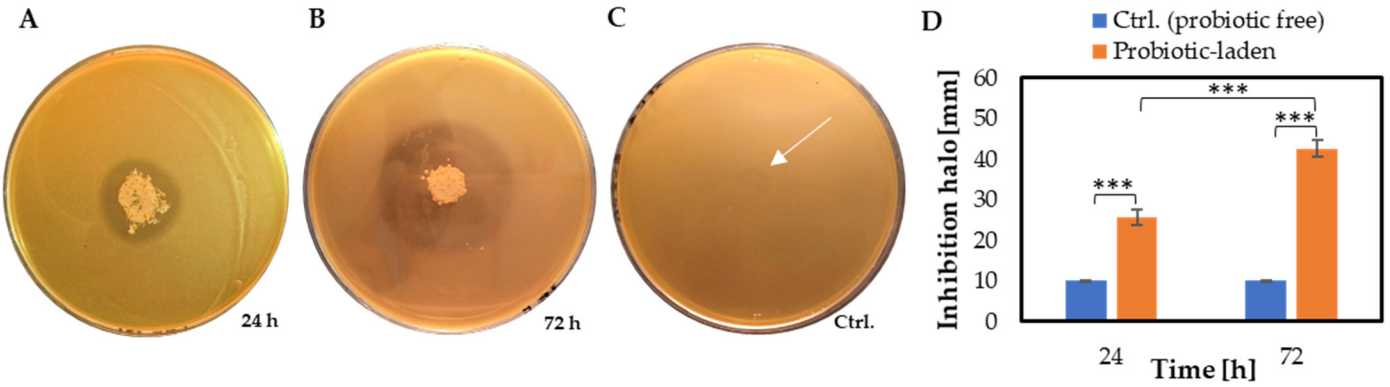

Figure 10. Ability of probiotic-loaded microparticles, visible as a white spot in the center of the plate, to inhibit *E. coli* growth. (**A**–**C**) Example photographs showing microparticles on plates covered by *E. coli*: (**A**) inhibition zone (i.e., clear halo) following 24 h incubation of the probiotic-loaded microparticles; (**B**) inhibition zone following 72 h of incubation of the probiotic-loaded microparticles; (**C**) control plate "Ctrl". In which probiotic-free microparticles were added. (**D**) Bar graph showing mean values of the diameters of the inhibition zones ± standard error of the mean. The diameters of the unloaded spots, barely visible, were approximately 10 mm (arrow in (**C**)). *** $p < 0.001$, ANOVA test.

4. Discussion

The alarming phenomenon of antimicrobial resistance has strongly highlighted that the use of antibiotics to treat upper respiratory tract-related diseases, such as OM, may not be resolutive. Currently, the annual incidence of acquired cholesteatoma is in the range of 9.0–12.6 cases per 100,000 adults and 3–15 cases per 100,000 children [3,4,28–30]. The topical treatments are unable to provide a complete cure of OM; rather, they are used to control preoperative infection or inflammation and to reduce the risk of postoperative complications [31,32]. To avoid surgery, patients and otologists place great hope in new biotechnological treatments. Bacteriotherapy, which relies on the administration of probiotics to compete with the infectious pathogens, has been recently emerging as an attractive option in this scenario [33].

This study aimed to harness the potential of bacteriotherapy by developing an SA-based probiotic-laden delivery system. The combination of electrosprayed SA microparticles and electrospun SA/PEO ultrafine fibers served as a supportive substrate for topical application to the tympanic membrane to address middle ear infections. In this research, SA was chosen as a suitable material to obtain the desired formulations. SA, a linear polysaccharide derived from algae, possesses advantageous properties, including high water-retention capacity, biocompatibility in many body settings, non-immunogenicity and tunable mechanical properties [34–36]. SA solutions can form physically crosslinked gels

in the presence of divalent ions like Ca^{2+}, thus enabling the creation of solid structures that can be ideal for probiotic-laden solutions, by avoiding their exposure to potentially harmful conditions, like toxic chemicals or UV radiation [36].

The use of the electrospray technique allowed the production of consistent batches of SA microparticles, both probiotic free and probiotic laden. These microparticles exhibited spherical or slightly elliptical shapes with narrow diameter distributions, measuring in the hundreds of microns (i.e., 346.5 ± 10.0 µm and 395.5 ± 23.5 µm for probiotic-free and probiotic-laden microparticles, respectively). Electrospray mild operating conditions hold great potential for encapsulating live cells within biopolymeric networks, making it a viable method for targeted bacterial delivery to specific body sites. Notably, this approach aligns with recent studies that have successfully employed electrospray for the encapsulation of live bacteria, as seen in the work of Zaeim et al., involving hydrogel microspheres encapsulating *Lactobacillus plantarum* [17]. The produced microparticles were demonstrated to be easily collected by filtration and to act as effective carriers for the gradual and sustained release of encapsulated agents through various administration routes. In our case, the produced microparticles exhibited outstanding stability and minimal biodegradation under simulated biological condition. These characteristics make them suitable for formulations that require the gradual and controlled release of encapsulated agents, particularly in the context of chronic diseases with a challenging healing process.

Electrospinning is a simple technique widely used in the biomedical field [37]. However, electrospinning of pure SA presents inherent difficulties, due to the stiff molecular structure of the SA, the high electrical conductivity of the SA aqueous solution resulting from its polyelectrolytic nature, and the formation of SA intra- and inter-molecular hydrogen bonds. These aspects contribute to the high-surface tension of SA, making the electrospinning process challenging [38]. Although the literature lacks reports of successful electrospinning of aqueous solutions of pure SA, some studies have employed co-solvents or carrier polymers to address this issue [38–40]. Nie et al. demonstrated the production of uniform SA fibers in the submicron range using glycerol as a strong polar co-solvent [40]. Glycerol ability to enhance the entanglements of SA chains by forming new hydrogen bonds, proved crucial in improving the electro-spinnability. However, this approach had limitations, including the presence of spherical clusters on the fiber surface and wide diameter distributions.

The other well-explored approach to facilitate SA electrospinning process involves the incorporation of hydro-soluble polymers, such as PVA and PEO, as carrier materials [35]. Saquing et al. investigated SA/PEO blends and found that PEO played a pivotal role in enhancing electrospinning by increasing viscosity and relaxation time, while lowering the conductivity and surface tension of the solution [39]. To achieve uniform fiber formation, a minimum PEO molecular weight of 600 kDa was required, while a higher molecular weight PEO (i.e., 1000–2000 kDa) enabled the production of fibers with greater SA content and larger diameters. The addition of 1% Triton X-100, a non-ionic surfactant, revealed to be beneficial to improve SA content, reaching a maximum of 85%.

In this research, SA electrospinning challenges were addressed by utilizing high molecular weight PEO (i.e., 1000 kDa) as a support polymer, ensuring high SA content in the resulting fibers (i.e., 7 w% SA51MG03 + 3 w% PEO). To further enhance the electrospinnability and promote defect-free structure formation, Triton X-100 was also introduced. The successful electrospinning of SA/PEO solution was corroborated by the results of the rheological studies, which had a weak shear-thinning behavior, crucial for preventing the disruption of entanglements and promoting fiber elongation during the electrospinning process. The Hagen–Poiseuille equation calculated a shear rate within the Newtonian region, further underscoring the suitability of this approach [26]. The SA/PEO solution yielded continuous ultrafine fibers, with diameters of 264 ± 95 nm and 281 ± 79 nm, when collected at rotation speeds of 60 rpm and 1500 rpm, respectively. Optimal fiber morphology was best maintained when crosslinking was carried out by mixing 2 w/v% $CaCl_2$ in a 30/70 v/v% ethanol/dH_2O reticulation bath. Since the crosslinking solution

was water based, PEO could be dissolved, allowing the fabrication of SA fibers. However, the fiber diameters increased (i.e., 404 ± 10 nm and 434 ± 92 nm for collection speeds of 60 rpm and 1500 rpm, respectively). This outcome is consistent with evidence reported in the literature, where the simultaneous and competing influence of PEO removal and SA crosslinking gave rise to an overall increase in fiber size [41]. Furthermore, the presence of ethanol in the crosslinking bath expedited the crosslinking of SA fibers, by accelerating the formation of solid fiber mashes while also enhancing the fibers' swelling behavior [42–44].

After 24 h in DPBS, a remarkable increase in fiber diameters was observed (i.e., 853 ± 22 nm and 666 ± 14 nm for collection speeds of 60 rpm and 1500 rpm, respectively). This phenomenon can be attributed to the swelling behavior of the fibers combined with the morphological changes that occurred after crosslinking. The fusion of individual fibers resulted in a larger size, with an overall reduction in the surface area of the final fibrous mashes, potentially leading to delayed biodegradation during the soaking tests. Combining these probiotic-laden SA microparticles with an SA/PEO fiber web led to the obtainment of an SA-based system, in the form of a patch, able to entrap and position probiotics at a specific body site, such as the middle ear and/or the eardrum. Additionally, the patch components were cytocompatible with human dermal keratinocytes, found on the outer auditory canal and on the external layer of the eardrum, which is promising for a future clinical translation. Lastly, we obtained the first evidence of antimicrobial activity exerted by probiotic-laden microparticles towards *E. coli* using the soft agar overlay method. *E coli* was chosen as a model pathogen, as is found in OM isolates [45,46]. Although preliminary, the obtained findings highlighted a pronounced antimicrobial activity in vitro. This evidence demonstrates that the probiotics were viable after the electrospray encapsulation and were able to diffuse their products out of the microparticles for 72 h, which supports the bioactivity of the patch. Further in vitro studies will disclose the antimicrobial activity towards other pathogens relevant for middle ear infections, also considering advanced in vitro models (e.g., infected cells and tissues) and bioreactors. Future research directions could aim to evaluate in vivo if the local administration (i.e., nasal-pharyngeal/intra-aural/intra-tympanic) of beneficial bacteria or their products could have a positive impact on the eradication or control of infection and inflammation caused by common otopathogens of the middle ear, thus envisioning possible safe strategies for preventing or treating chronic OM.

By synergizing the entrapment capacity of the microparticles with the physico-mechanical properties of the ultrafine fibers, this innovative approach paves the way to novel strategies to restore and maintain the proper function of the middle ear microbiome [18]. Therefore, probiotic-loaded microparticles could hold promise in delivering probiotics or postbiotics to the upper respiratory tract, aiding in the restoration of site-specific microbiota and facilitating the healing process for OM.

5. Conclusions

This study aimed to investigate SA in producing an electrospun patch to deliver probiotics or postbiotics locally to the middle ear. The developed system incorporated probiotics into SA microspheres obtained via electrospray, which were subsequently inserted within SA/PEO fiber meshes to create a patch. The rheological behavior of the solutions was studied, and the swelling behavior of the produced fibers was evaluated. The patch resulted in being cytocompatible with HaCaT cells. In addition, the probiotics were viable and active against *E. coli* after encapsulation, which demonstrates the safety and effectiveness of the developed processing method. The developed strategy seems promising to produce 0D, 1D and 2D delivery systems for the treatment of chronic otitis media. However, further studies are necessary to improve the electro-spinnability of alginate and assess the efficacy of bacteriotherapy in in vivo models.

Author Contributions: Conceptualization, L.B. and S.D.; methodology, G.B., M.M. and S.D.; validation, R.R., B.C., G.B., M.M. and S.D.; formal analysis, R.R., B.C., L.Z., B.A., T.M. and S.E.; investigation, R.R., B.C., L.Z., B.A., T.M., E.K. and S.E.; resources, G.B. and S.D.; data curation, R.R., B.C. and L.Z.; writing—original draft preparation, R.R., B.C., M.M., G.B. and S.D.; writing—review and editing, R.R., G.B., L.Z., M.M. and S.D.; visualization, R.R., B.C., M.M. and S.D.; supervision, G.B., M.M. and S.D.; project administration, S.D.; funding acquisition, G.B. and S.D. All authors have read and agreed to the published version of the manuscript.

Funding: This research was funded by the Italian Ministry of University and Research (MIUR) under the framework Action II of PON "Ricerca e Innovazione" 2014–2020, project "Sviluppo di nutraceutici da fonti naturali—BIONUTRA" (CUP B14I20001320005), and by PNRR "THE—Tuscany Health Ecosystem"; Spoke 7—Innovating Translational Medicine-Sub-project 5—Innovative models for management of infections caused by antibiotic-resistant bacteria (Project code: ECS00000017; CUP I53C22000780001).

Institutional Review Board Statement: Not applicable.

Informed Consent Statement: Not applicable.

Data Availability Statement: Data are available from the corresponding author, upon reasonable request.

Acknowledgments: The authors thank Irene Anguillesi and Delfo D'Alessandro (University of Pisa) for their technical support for rheology and scanning electron microscopy analyses, respectively. The authors thank Linari s.r.l. for supporting the research activities.

Conflicts of Interest: The authors declare no conflict of interest.

References

1. Schilder, A.G.M.; Chonmaitree, T.; Cripps, A.W.; Rosenfeld, R.M.; Casselbrant, M.L.; Haggard, M.P.; Venekamp, R.P. Otitis Media. *Nat. Rev. Dis. Prim.* **2016**, *2*, 16063. [CrossRef]
2. Monasta, L.; Ronfani, L.; Marchetti, F.; Montico, M.; Vecchi Brumatti, L.; Bavcar, A.; Grasso, D.; Barbiero, C.; Tamburlini, G. Burden of Disease Caused by Otitis Media: Systematic Review and Global Estimates. *PLoS ONE* **2012**, *7*, e36226. [CrossRef] [PubMed]
3. Bluestone, C.D. Clinical course, complications and sequelae of acute otitis media. *Pediatr. Infect. Dis. J.* **2000**, *19* (Suppl. 5), S37–S46. [CrossRef] [PubMed]
4. Louw, L. Acquired Cholesteatoma Pathogenesis: Stepwise Explanations. *J. Laryngol. Otol.* **2010**, *124*, 587–593. [CrossRef] [PubMed]
5. Gavrilovici, C.; Spoială, E.-L.; Miron, I.-C.; Stârcea, I.M.; Halițchi, C.O.I.; Zetu, I.N.; Lupu, V.V.; Pânzaru, C. Acute Otitis Media in Children—Challenges of Antibiotic Resistance in the Post-Vaccination Era. *Microorganisms* **2022**, *10*, 1598. [CrossRef]
6. Horhat, R.; Horhat, F.-R.; Mocanu, V. Is Multidrug Resistance in Acute Otitis Media with Streptococcus Pneumoniae Associated with a More Severe Disease? *Med. Princ. Pract.* **2021**, *30*, 571–578. [CrossRef]
7. Murugaiyan, J.; Kumar, P.A.; Rao, G.S.; Iskandar, K.; Hawser, S.; Hays, J.P.; Mohsen, Y.; Adukkadukkam, S.; Awuah, W.A.; Jose, R.A.M.; et al. Progress in Alternative Strategies to Combat Antimicrobial Resistance: Focus on Antibiotics. *Antibiotics* **2022**, *11*, 200. [CrossRef]
8. van den Broek, M.F.L.; De Boeck, I.; Kiekens, F.; Boudewyns, A.; Vanderveken, O.M.; Lebeer, S. Translating Recent Microbiome Insights in Otitis Media into Probiotic Strategies. *Clin. Microbiol. Rev.* **2019**, *32*, 10-1128. [CrossRef]
9. Skovbjerg, S.; Roos, K.; Holm, S.E.; Håkansson, E.G.; Nowrouzian, F.; Ivarsson, M.; Adlerberth, I.; Wold, A.E. Spray Bacteriotherapy Decreases Middle Ear Fluid in Children with Secretory Otitis Media. *Arch. Dis. Child.* **2009**, *94*, 92–98. [CrossRef]
10. Hong, J.; Yeo, M.; Yang, G.H.; Kim, G. Cell-Electrospinning and Its Application for Tissue Engineering. *Int. J. Mol. Sci.* **2019**, *20*, 6208. [CrossRef]
11. Günday, C.; Anand, S.; Gencer, H.B.; Munafò, S.; Moroni, L.; Fusco, A.; Donnarumma, G.; Ricci, C.; Hatir, P.C.; Türeli, N.G.; et al. Ciprofloxacin-Loaded Polymeric Nanoparticles Incorporated Electrospun Fibers for Drug Delivery in Tissue Engineering Applications. *Drug Deliv. Transl. Res.* **2020**, *10*, 706–720. [CrossRef]
12. Azimi, B.; Ricci, C.; Macchi, T.; Günday, C.; Munafò, S.; Maleki, H.; Pratesi, F.; Tempesti, V.; Cristallini, C.; Bruschini, L.; et al. A Straightforward Method to Produce Multi-Nanodrug Delivery Systems for Transdermal/Tympanic Patches Using Electrospinning and Electrospray. *Polymers* **2023**, *15*, 3494. [CrossRef]
13. Danti, S.; Anand, S.; Azimi, B.; Milazzo, M.; Fusco, A.; Ricci, C.; Zavagna, L.; Linari, S.; Donnarumma, G.; Lazzeri, A.; et al. Chitin Nanofibril Application in Tympanic Membrane Scaffolds to Modulate Inflammatory and Immune Response. *Pharmaceutics* **2021**, *13*, 1440. [CrossRef]
14. Diep, E.; Schiffman, J.D. Electrospinning Living Bacteria: A Review of Applications from Agriculture to Health Care. *ACS Appl. Bio Mater.* **2023**, *6*, 951–964. [CrossRef]

15. Kurečič, M.; Rijavec, T.; Hribernik, S.; Lapanje, A.; Kleinschek, K.S.; Maver, U. Novel Electrospun Fibers with Incorporated Commensal Bacteria for Potential Preventive Treatment of the Diabetic Foot. *Nanomedicine* **2018**, *13*, 1583–1594. [CrossRef] [PubMed]
16. Nagy, Z.K.; Wagner, I.; Suhajda, Á.; Tobak, T.; Harasztos, A.H.; Vigh, T.; Sóti, P.L.; Pataki, H.; Molnár, K.; Marosi, G. Nanofibrous Solid Dosage Form of Living Bacteria Prepared by Electrospinning. *eXPRESS Polym. Lett.* **2014**, *8*, 352–361. [CrossRef]
17. Zaeim, D.; Sarabi-Jamab, M.; Ghorani, B.; Kadkhodaee, R.; Tromp, R.H. Electrospray Assisted Fabrication of Hydrogel Microcapsules by Single-and Double-Stage Procedures for Encapsulation of Probiotics. *Food Bioprod. Process.* **2017**, *102*, 250–259. [CrossRef]
18. Rovelli, R.; Cecchini, B.; Zavagna, L.; Azimi, B.; Ricci, C.; Esin, S.; Milazzo, M.; Batoni, G.; Danti, S. Emerging Multiscale Biofabrication Approaches for Bacterio-Therapy. *Molecules* **2023**. *under review*. [CrossRef]
19. Aduba Jr, D.C.; Yang, H. Polysaccharide Fabrication Platforms and Biocompatibility Assessment as Candidate Wound Dressing Materials. *Bioengineering* **2017**, *4*, 1. [CrossRef]
20. Coltelli, M.-B.; Danti, S.; De Clerck, K.; Lazzeri, A.; Morganti, P. Pullulan for Advanced Sustainable Body-and Skin-Contact Applications. *J. Funct. Biomater.* **2020**, *11*, 20. [CrossRef]
21. Lee, K.Y.; Mooney, D.J. Alginate: Properties and Biomedical Applications. *Prog. Polym. Sci.* **2012**, *37*, 106–126. [CrossRef] [PubMed]
22. Abourehab, M.A.S.; Rajendran, R.R.; Singh, A.; Pramanik, S.; Shrivastav, P.; Ansari, M.J.; Manne, R.; Amaral, L.S.; Deepak, A. Alginate as a Promising Biopolymer in Drug Delivery and Wound Healing: A Review of the State-of-the-Art. *Int. J. Mol. Sci.* **2022**, *23*, 9035. [CrossRef] [PubMed]
23. Diep, E.; Schiffman, J.D. Encapsulating Bacteria in Alginate-Based Electrospun Nanofibers. *Biomater. Sci.* **2021**, *9*, 4364–4373. [CrossRef] [PubMed]
24. Gorroñogoitia, I.; Urtaza, U.; Zubiarrain-Laserna, A.; Alonso-Varona, A.; Zaldua, A.M. A Study of the Printability of Alginate-Based Bioinks by 3D Bioprinting for Articular Cartilage Tissue Engineering. *Polymers* **2022**, *14*, 354. [CrossRef]
25. Jeoh, T.; Wong, D.E.; Strobel, S.A.; Hudnall, K.; Pereira, N.R.; Williams, K.A.; Arbaugh, B.M.; Cunniffe, J.C.; Scher, H.B. How Alginate Properties Influence in Situ Internal Gelation in Crosslinked Alginate Microcapsules (CLAMs) Formed by Spray Drying. *PLoS ONE* **2021**, *16*, e0247171. [CrossRef]
26. Yarin, A.L.; Koombhongse, S.; Reneker, D.H. Taylor Cone and Jetting from Liquid Droplets in Electrospinning of Nanofibers. *J. Appl. Phys.* **2001**, *90*, 4836–4846. [CrossRef]
27. Shokryazdan, P.; Sieo, C.C.; Kalavathy, R.; Liang, J.B.; Alitheen, N.B.; Faseleh Jahromi, M.; Ho, Y.W. others Probiotic Potential of Lactobacillus Strains with Antimicrobial Activity against Some Human Pathogenic Strains. *BioMed Res. Int.* **2014**, *2014*, 927268. [CrossRef]
28. Kemppainen, H.O.; Puhakka, H.J.; Laippala, P.J.; Sipilä, M.M.; Manninen, M.P.; Karma, P.H. Epidemiology and Aetiology of Middle Ear Cholesteatoma. *Acta Otolaryngol.* **1999**, *119*, 568–572.
29. de Aquino, J.E.A.P.; Cruz Filho, N.A.; Aquino, J.N.P. de Epidemiology of Middle Ear and Mastoid Cholesteatomas: Study of 1146 Cases. *Braz. J. Otorhinolaryngol.* **2011**, *77*, 341–347. [CrossRef]
30. Nelson, M.; Roger, G.; Koltai, P.J.; Garabedian, E.-N.; Triglia, J.-M.; Roman, S.; Castellon, R.J.; Hammel, J.P. Congenital Cholesteatoma: Classification, Management, and Outcome. *Arch. Otolaryngol. Head. Neck Surg.* **2002**, *128*, 810–814. [CrossRef]
31. Vital, V. Pediatric Cholesteatoma: Personal Experience and Review of the Literature. *Otorhinolaryngol. Head Neck Surg.* **2011**, *45*, 5–14.
32. Pierce, N.E.; Antonelli, P.J. Efficacy of Antibiotic Prophylaxis Prior to Tympanoplasty for Contaminated Cholesteatoma. *Laryngoscope* **2016**, *126*, 2363–2366. [CrossRef] [PubMed]
33. Folino, F.; Ruggiero, L.; Capaccio, P.; Coro, I.; Aliberti, S.; Drago, L.; Marchisio, P.; Torretta, S. Upper respiratory tract microbiome and otitis media intertalk: Lessons from the literature. *J. Clin. Med.* **2020**, *9*, 2845. [CrossRef] [PubMed]
34. dos Santos, L.A. Natural Polymeric Biomaterials: Processing and Properties. In *Reference Module in Materials Science and Materials Engineering*; Elsevier: Amsterdam, The Netherlands, 2017; pp. 1–5.
35. Sachan, N.K.; Pushkar, S.; Jha, A.; Bhattcharya, A. Sodium Alginate: The Wonder Polymer for Controlled Drug Delivery. *J. Pharm. Res* **2009**, *2*, 1191–1199.
36. Hecht, H.; Srebnik, S. Structural Characterization of Sodium Alginate and Calcium Alginate. *Biomacromolecules* **2016**, *17*, 2160–2167. [CrossRef] [PubMed]
37. Maleki, H.; Azimi, B.; Ismaeilimoghadam, S.; Danti, S. Poly (Lactic Acid)-Based Electrospun Fibrous Structures for Biomedical Applications. *Appl. Sci.* **2022**, *12*, 3192. [CrossRef]
38. Mokhena, T.C.; Mochane, M.J.; Mtibe, A.; John, M.J.; Sadiku, E.R.; Sefadi, J.S. Electrospun Alginate Nanofibers toward Various Applications: A Review. *Materials* **2020**, *13*, 934. [CrossRef]
39. Saquing, C.D.; Tang, C.; Monian, B.; Bonino, C.A.; Manasco, J.L.; Alsberg, E.; Khan, S.A. Alginate-Polyethylene Oxide Blend Nanofibers and the Role of the Carrier Polymer in Electrospinning. *Ind. Eng. Chem. Res.* **2013**, *52*, 8692–8704. [CrossRef]
40. Nie, H.; He, A.; Zheng, J.; Xu, S.; Li, J.; Han, C.C. Effects of Chain Conformation and Entanglement on the Electrospinning of Pure Alginate. *Biomacromolecules* **2008**, *9*, 1362–1365. [CrossRef]
41. Leung, V.; Hartwell, R.; Elizei, S.S.; Yang, H.; Ghahary, A.; Ko, F. Postelectrospinning Modifications for Alginate Nanofiber-Based Wound Dressings. *J. Biomed. Mater. Res. Part B Appl. Biomater.* **2014**, *102*, 508–515. [CrossRef]

42. Yoo, S.M.; Ghosh, R. A Method for Coating of Hollow Fiber Membranes with Calcium Alginate. *J. Memb. Sci.* **2018**, *558*, 45–51. [CrossRef]
43. Chang, J.-J.; Lee, Y.-H.; Wu, M.-H.; Yang, M.-C.; Chien, C.-T. Preparation of Electrospun Alginate Fibers with Chitosan Sheath. *Carbohydr. Polym.* **2012**, *87*, 2357–2361. [CrossRef]
44. Hassan, R.M.; Zaafarany, I.A.; Gobouri, A.A.; Fawzy, A.; Takagi, H.D. Polymeric Biomaterial Hydrogels: II. Behavior of Some Coordination Biopolymeric Metal-Alginate Ionotropic Hydrogels in Aqueous Solutions. *J. Life Medcine* **2014**, *1*, 41–47. [CrossRef]
45. Chanin, A. *E coli*. Otitis Media. *JAMA* **1971**, *217*, 826. [CrossRef]
46. Afolabi, O.A.; Salaudeen, A.G.; Ologe, F.E.; Nwabuisi, C.; Nwawolo, C.C. Pattern of Bacterial Isolates in the Middle Ear Discharge of Patients with Chronic Suppurative Otitis Media in a Tertiary Hospital in North Central Nigeria. *Afr. Health Sci.* **2012**, *12*, 362–367. [CrossRef]